BOLETIN DE LA SOCIEDAD ESPAÑOLA DE
Cerámica y Vidrio
A R T I C U L O

Dynamic fracture and fragmentation patterns of borosilicate laminate glasses

F. ORGAZ [1], T. GÓMEZ-DEL RÍO [2]

[1] Instituto de Cerámica y Vidrio, C/ Kelsen, nº 5, 28049 Madrid (Spain)
[2] Departamento de Ciencia e Ingeniería de Materiales, Universidad Rey Juan Carlos, C/Tulipán s/n, 28933 Móstoles, Madrid (Spain)

The dynamic behaviour of laminate borosilicate glasses (BSG) with polyvinylbutiral (PVB) interfaces (0,38 mm) located at different distances from the impact point have been studied and compared with monolithic glass. The mechanical behaviour under impact loads have been studied using a compression split Hopkinson pressure bar (SHPB). In these experiments, the stress-strain curves of the materials at high loading rates and the capability of transmitting and reflecting the impact energy have been determined. The influence of the position of the interface on the fragmentation statistics of the SHPB recovered fragments has also been considered and analysed according to the published theoretical models.

Keywords: laminate borosilicate glasses; split Hopkinson pressure bar; mechanical properties; fragmentation analysis.

Fractura dinámica y patrones de fragmentación de vidrios laminados de borosilicato

En este trabajo se ha estudiado los comportamientos dinámicos de un vidrio monolítico de borosilicato y varios laminados de cristal de borosilicato (BSG) con intercaras de polyvinylbutiral (PVB) (0,38 mm) situados a diferentes distancias respecto del punto de impacto. Los resultados de las diferentes configuraciones de laminados se han comparado con el vidrio monolítico. El comportamiento mecánico bajo cargas de impacto se han estudiado realizando ensayos de compresión con una barra Hopkinson (SHPB). A partir de estos experimentos se obtienen las curvas tensión-deformación de los materiales a altas velocidades de carga y su capacidad de transmitir y reflejar la energía del impacto. La influencia de la posición de la interfaz en las estadísticas de la fragmentación de los fragmentos recuperados también se ha considerado y analizado de acuerdo a los modelos teóricos publicados.

Palabras clave: laminado de vidrio de borosilicato, barra Hopkinson; propiedades mecánicas; análisis de fragmentación

1. INTRODUCTION

Transparent armours are receiving recent attention due to new threats which require better security conditions. Weight and thickness seem to be the limiting factors in armour manufacture [1, 2, 3]. As the extent of protection required increases, so does the thickness of the armour plate and the associated weight. This is problematic in the design of transparent armour because it is well known that with increasing thickness of transparent material, light transmission decreases [4, 5]. When a projectile impacts a glass or ceramic tile at high speed, a compressive stress wave is created which propagates from the impacted area in the impact direction. When this wave reaches the rear face of the tile, it is partially reflected as a tensile stress wave producing cracking and fragmentation of the glass material [2]. Ballistic performance of ceramic and glass materials depends on a number of properties. Ceramics and glasses should have high hardness values in order to defeat a projectile and to decrease its velocity, but the crack propagation after impact should not be intensive. In general, the penetrator is distorted and eroded during the initial contact with the material and the erosion of the penetrator is greater as the hardness of the material increases. While there is no direct correlation to a single physical or mechanical property for improved ballistic performance, high hardness, strength, and toughness are desirable. The ballistic energy dissipation ability D can be then calculated by the equations [6]:

$$D = \frac{0.36(Hv \cdot E \cdot c)}{K_{IC}^2} = 0.36 \cdot c \cdot B \qquad (1)$$

where Hv is the Vickers hardness, K_{Ic} the fracture toughness, E the Young's modulus, c the sonic velocity and B the brittleness factor,

$$B = \frac{Hv \cdot E}{K_{IC}^2} \qquad (2)$$

Manufacture of transparent armours follows the principles well established for the opaque ones. Armour against advanced threats has typically structure of laminates. In traditional laminate glass armour, the projectile strike face is made of glass. The strike face is then laminated to other

sheets of glass using well known interlayers to increase the thickness of the system. The final layer is composed of a thicker polymer layer. The role of the backing layer is to catch residual projectile fragments and comminuted particles and together with interlayers to hinder the crack propagation. Stiff and tough material, such as polycarbonate, is typically used for this layer. These systems can be quite thick and heavy due to the amount of glass needed to stop high powered projectiles [4]. Comprehensive testing of glass–polycarbonate laminates with so-called armour piercing (AP) ammunitions, i.e. projectiles with a hard core material (steel, tungsten carbide or tungsten), has demonstrated that the core of the projectiles is hardly being eroded during penetration and does not break in most instances. Thus, targets of relatively high weight and thickness are needed in order to defeat AP threats with the traditional materials for transparent armour. A significant weight reduction can be achieved by means of a hard front layer of transparent ceramics. The front-face layer should be as hard as possible to damage the projectile in maximum range. In ideal case it should be harder than the projectile core. Glasses or glass ceramics are usually applied for internal layers. For high protection level relatively high armour thickness is needed, which subsequently results in high armour weight. If high protection level is requested, installation of these armours into armoured vehicles and objects is problematic because of their high thickness and weight. The problem of high thickness and weight of transparent armours is presently solved by research and development of new high hardness transparent materials. The four leading strike-face ceramic materials used in transparent armours are sapphire (single crystal alumina, Al_2O_3), aluminum oxynitride [sintered and HIP'd AlNx .(Al_2O_3)1-x], and spinel (sintered and HIP'd $MgAl_2O_4$) [7]. So far, certain technical and economic drawbacks impede the implementation of these hard front face transparent ceramic materials. Complementary strategies have been addressed to enhance the weak point of present transparent armours such as some kinds of hardened borosilicate glass, glass ceramics, new PU foils, low friction coatings, front face reflective layers, in order to dissipate the high kinetic energy (KE) associated to the impact [4].

The fundamental understanding of the mechanisms by which ceramic and glasses materials deform and fracture during dynamic impact loading has been advanced tremendously by the development, modification and augmentation of such techniques as Taylor impact, split-Hopkinson bar (SHPB), plate impact, explosive cylinder and spherical cavity expansion. A review has been recently published [8] on the dynamic fracture of ceramics in the framework of the ceramic armour penetration processes. The split Hopkinson bar is being widely used to determine the dynamic compressive strength of ceramics, glass and composites. Pulse shaping techniques to obtain compressive strain-stress data for testing brittle materials with SHPB were developed by Frew et al [9]. Stachler et al [10] used SHPB tests to study the failure of a high strength of alumina at strain rates of the order of 1000 s^{-1}. Dynamic fracture under multi-axial stresses has been studied by Nie and Chen [11] using cuboid borosilicate glass specimens with the material axis inclining to the loading direction at different angles. Recent investigations have also been addressed to visualize the origin, growth, coalescence and propagation of cracks produced by SHPB experiments in confined and unconfined materials. High speed photographs were correlated in time with measurements of the stresses in the sample [12-13 , 9].

The objective of the present work is to better understand the dynamic behaviour of borosilicate laminate glasses with PVB foils located at different distances from the impact and compared with monolithic glasses. For this reason, dynamic compression tests have been carried out using a Hopkinson bar, and the energy reflected, transmitted and absorbed in each case has been calculated. Because the fracture and pulverization of the ceramic material are effective ways to dissipate part of the incident energy generated by the impact, it is expected that from the statistical distribution function and from the morphology of the pulverized fragments and their causing energies, relevant information can be drawn on the factors governing the impact and penetration resistance of these materials. The ultimate goal is to use the results of these non-ballistic experiments to determine constitutive constants and governing factors for material models, with application to transparent armour design.

2. EXPERIMENTAL PROCEDURE

2.1. Materials

Different laminates of commercial borosilicate (Schott) / PVB interfaces samples summarized in Figure.1 were tested.

Apart from the borosilicate monolithic considered as the baseline configuration, a PVB interlayer located at different positions have been analyzed. For the first variant, a PVB interlayer was carried to the mid-length of the borosilicate component. For the second variant, this interlayer is carried nearer to the impact face (in a 2:8 laminate) and in the third variant, the interlayer is located 2/8 away from the back side of the specimen. To minimize the end friction effects, the specimens-contacting surfaces in compression tests in the Hopkinson bar were lubricated before mechanical loading. The specimens used in this characterization were cylinders with a diameter of 6 mm and total thickness ranging between 10 and 11 mm.

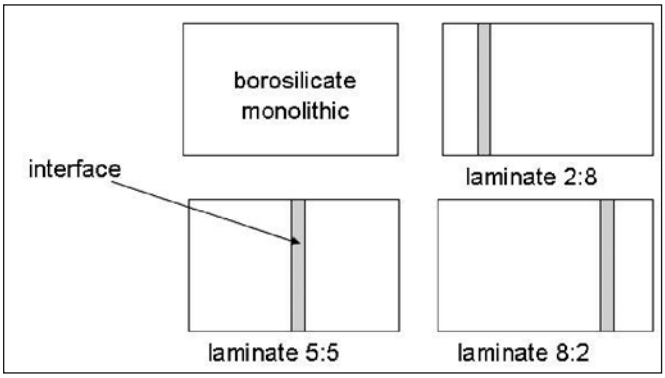

Figure 1. Scheme of the borosilicate and the three different laminates with the interface located at different places

2.2. The SPHB set up

The experimental procedure is focused on reproducing as much as possible the conditions presented in a ballistic impact problem. For this reason, dynamic compression tests have been carried out using a split Hopkinson pressure bar (SPHB), which is a technique to characterize materials at high strain rates. The SPHB device is described in more detail elsewhere [14]. The SPHB device consists of a gas gun, an input bar and an output bar, the supports, and the data acquisition system. Both bars are made of steel, 20 mm in diameter and lengths of 1.2 m and 0.8 m for the input and output bars, respectively (Fig. 2).

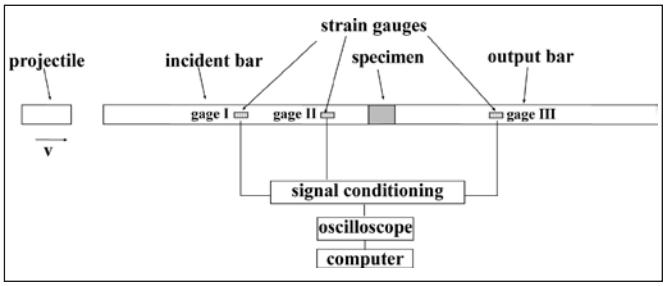

Figure 2. Schematic representation of the SHPB setup.

The air gun impels a projectile against the input bar where, as a consequence of the impact, a compression pulse is generated. It travels along the input bar up to the specimen, where is partially reflected and partially transmitted to the output bar. To measure the incident, reflected and transmitted pulses, strain gauges (VISHAY J2A-06-S047K-350) are attached to the bars. The strain gage signals are recorded using a VISHAY 2200 conditioner together with a TEKTRONIX TDS 420A digital oscilloscope. Assuming that both bars behave elastically, measurements of strains in the bars provide the dynamic stress-strain curve of the specimen material or the energy reflected and transmitted in the bar/specimen interface, according to the following expressions [15]:

$$\sigma_p(t) = \frac{EA_b}{A_s}\cdot\varepsilon_T(t) \qquad \varepsilon_p(t) = \int_0^t \frac{2c}{l}\cdot\varepsilon_R(t)dt \quad (3)$$

$$E_R = \frac{1}{2}EA_bc\int_0^t \varepsilon_R^2(t)\,dt \qquad E_T = \frac{1}{2}EA_bc\int_0^t \varepsilon_T^2(t)\,dt \quad (4)$$

where $\sigma_p(t)$ and $\varepsilon_p(t)$ are the stress and strain in the specimen; $\varepsilon_R(t)$ and $\varepsilon_T(t)$ the strain in the bars corresponding to the reflected and transmitted wave; A_s and l the section and length of the specimens; A_b, E and c the section, Young's modulus and wave velocity of the bars; and finally E_R and E_T the energy reflected and transmitted by the specimen, respectively. Dynamic uniaxial compression tests were conducted at high strain rates of about 800-1200 s^{-1}

3. SHPB RESULTS AND DISCUSSION

Layered structures have been studied for developing armour systems. However the analysis of the effect of the distance to the impact face of the interlayer is not well understood. The approach of this study was to use the Hopkinson bar to perform impact tests and verified which location of the interlayer inside the glass material behaves better, this is, reflects and absorbs more percentage of the incident impact energy. Figure 3 shows the original oscilloscope wave records of the sample 2:8 subjected to a dynamic compressive test with the Hopkinson bar. A high amplitude of the reflected wave and a low amplitude of the transmitted wave is observed.

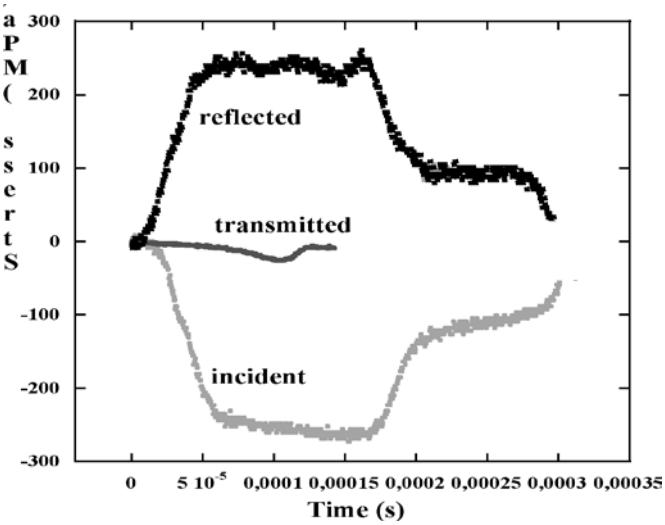

Figure 3. Stress waves recorded in an experiment (incident, transmitted and reflected).

Following the ideas presented in the introduction, the capability of the different laminates studied to reflect or transmit the impact energy is summarized in Table 1.

TABLE I. ENERGIES INCIDENT, REFLECTED AND TRANSMITTED CALCULATED FROM THE WAVES RECORDED USING EQUATION 4. PERCENTAGES OF ENERGIES REFLECTED, TRANSMITTED AND ABSORBED HAVE ALSO BEEN INCLUDED.

Samples	Borosilicate monolithic	Laminate 2:8	Laminate 5:5	Laminate 8:2
Incident energy (J)	42,93	41,23	40,11	36,41
Reflected energy (J)	21,87	38,05	34,83	34,86
Transmitted energy (J)	1,47	0,11	0,15	0,11
Reflected energy (%)	50,95	92,31	86,84	95,73
Transmitted energy (%)	3,42	0,26	0,38	0,31
Absorbed energy (%)	45,63	7,59	13,01	4,15

It is considered that all the incident energy is spent in reflected, transmitted and absorbed energies. So, the percentage of energies is calculated assuming there is no friction or energy lost. Two conclusions can be clearly derived: the borosilicate monolithic reflects much less energy than any of the interlayer laminates; but it absorbs more than any of the others. Also, the nearer the PVB is to the impact side, the smaller the energy transmitted. Unlike that, the characteristic stress, there are not appreciable differences between the different laminates.

Figure 4 shows the stress-strain curves of the monolithic borosilicate (4a) and borosilicate with interlayer of PVB in laminate 5:5 (4b). The curves obtained applying the typical

equations of SPHB presented before (eq. 3) have no meaning as the specimens tested are combination of different materials (except in the case of borosilicate monolithic specimen). This stress is always obtained directly form the transmitted wave measured in the output instrumented bar, because this is the usual and more accurate way to determine the stress in the specimen in the Hopkinson bar experiments. It should be noted that the maximum value reached by the stress in the dynamic tests does not represent any material failure, but it can be used as a parameter to measure, in some extend, the dynamic response of the laminate. The monolithic samples showed a higher yield stress and a lower strain than the laminated samples. The dynamic stress-strain curves are similar for all the laminates tested.

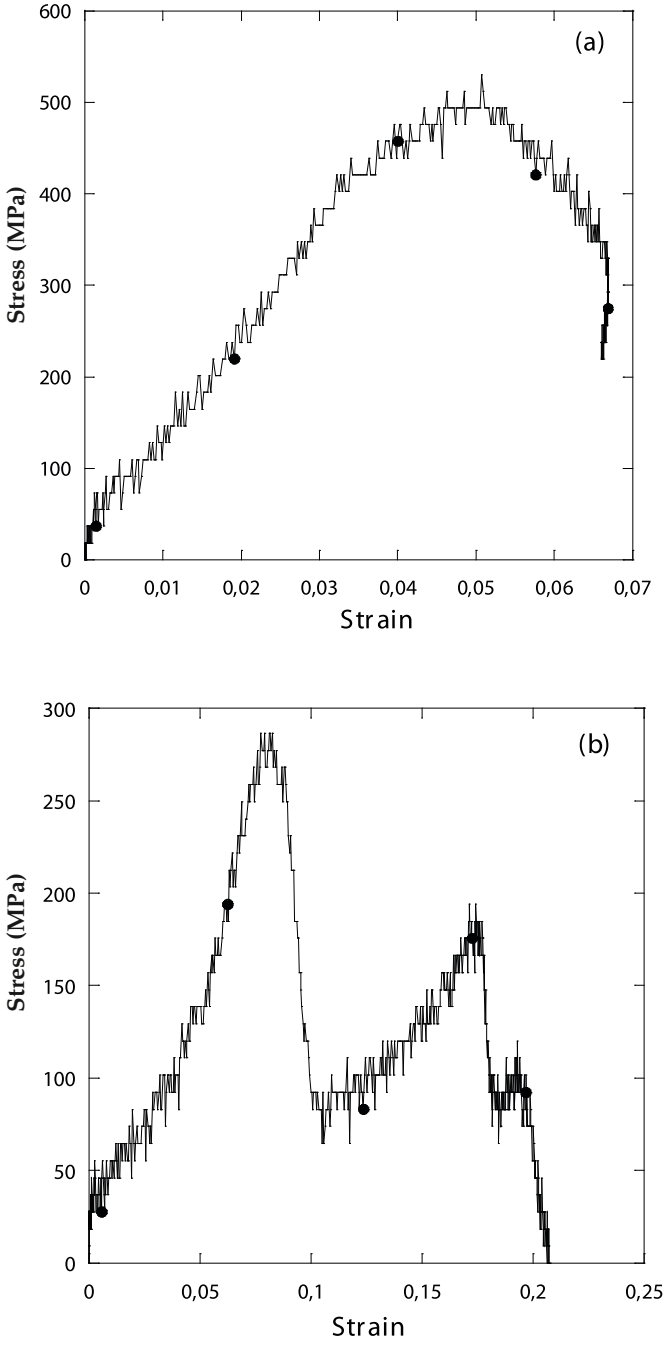

Figure 4. Dynamic stress-strain curves for monolithic borosilicate (a) and borosilicate with interlayer of PVB in laminate 5:5 (b).

4. DYNAMIC FRAGMENTATION. PATTERNS AND MODELING.

4.1 Experimental procedure

Post-mortem analysis of the fractured samples after being tested with the Hopkinson bar was performed by analysing the fragmentation size Distribution of fragment sizes was characterized through sieving techniques where the particles are classified in terms of their ability or inability to pass through an aperture of controlled size. SHPB recovered fragments were introduced onto a stack of sieves with successively finer apertures below and agitated by mechanical pulses to induce translation. Sieves with apertures of 50,100, 315, 630, 1000 and 2000 microns were used. After meshing, the direct measurement of the mass of each fraction of fragments was weighted.. For the specimens analyzed, the total weight of the fragments was around M $\approx$ 0,30 g. All the fragments were considered spherical because the precision of sieve analysis depends somewhat on the aspect ratio of the particle.

4.2. Results and discussion

The measured distributions of recovered fragments are shown in Fig. 5 which represents the cumulative weight of fragments with size > n as a function of the fragment size, n. As observed, larger fragments were recovered from laminated in comparison to monolithic BSG, which can be explained as due to a lower rupture stress and a higher toughness of the laminates.

Another important aspect to be considered is the relation between the energies involved during the dynamic impact tests and the level of fragmentation and pulverization produced, as analysed later on. A nearly linear relationship between average fragment size, L, and SHPB reflected energy (%) is observed in Figure 6. The average fragment size was calculated from the value at which the cumulative weight of fragments is 50% (Figure 5).

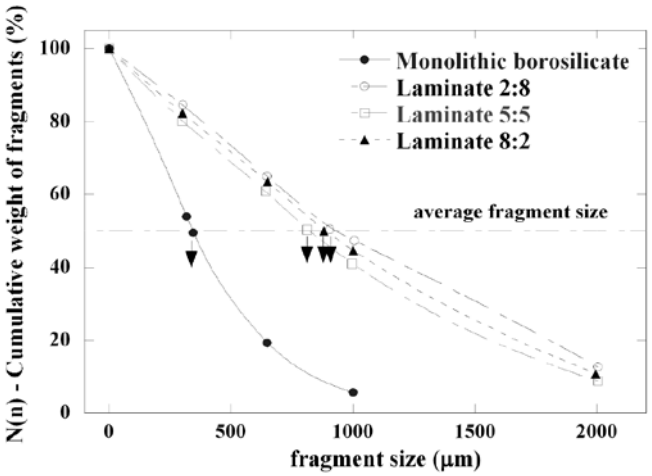

Figure 5. Cumulative weight of SHPB recovered fragments as a function of the fragment size.

Substantial progress has been made in the theoretical and numerical treatment of fragmentation, and especially in the cohesive treatment of the initiation, propagation, and coalescence of microcracks. Subhash et al [16] have reviewed recent advances in fragmentation modelling. The fragmentation under dynamic conditions involves the nucleation, growth, and coalescence of a network of cracks[17] which depend on the loading rates [18] and significantly influenced by the microscopic heterogeneities, microstructure [19] and on the nature and configuration of the materials and systems. Lienau [20], Mott and Linfoot [21], Grady and Kipp [22] and Grady [23] have proposed models based on statistical assumptions. Mott and Linfoot proposed the seminal work on fragmentation in the classified literature and later in the open literature. They forwarded a geometric statistics-based theory of fragmentation based on the random creation of cracks and their interaction through unloading waves to explain the fragment size distribution observed in dynamically expanding rings. One of the central assumptions of this work is that energy requirement in the actual fracture process is negligible and that fracture is instantaneous while Griffith assumed that all available energy is used up in creating free surfaces. According to Mott and Linfoot, the cumulative number of fragments N(n) is described by:

$$N(m) = N_0 e^{-(3N_0 m)^{1/3}} \quad (5)$$

or

$$N(n) = N_0 e^{-(2\lambda n)^{1/2}} \quad (6)$$

where K is the total number of fragments, n is the fragment area, and λ is a fitting parameter given by Ck=A with A denoting the total area of fragments and C a constant. Grady and Kipp [23] have further improved the models. They assume that the probability of fracture is spatially uniform and that all points in a body are accessible to fracture, and adjacent fracture sites can be arbitrarily close to each other. In application, an event can be regarded as continuous if the average fragment size is large relative to the minimum fragment size. For the specimens analyzed here, the minimum fragment size is typically less than one-fourth of the average fragment size. Thus, the assumption of continuous fracture is valid. Under such conditions, they have obtained the following distribution function for dynamic fragmentation:

$$N(m) = N_0 e^{\left(\frac{M}{\mu}-1\right)\ln\left(1-\frac{m}{M}\right)} \quad (7)$$

where M is the total mass of the body and μ the average fragment mass.

Grady and Kipp (23) have also proposed energy-based models in terms of the propagation of the microcracks and their interaction and coalescence during the fragmentation event. Their models rely on an energy balance between the surface energy released due to fracture and the kinetic energy of the generated fragments, and provides a simple relation between the average fragment size L and the strain rate $\dot{\varepsilon}$ as

$$L = 24^{1/3}\left(\frac{K_{IC}}{\rho c \dot{\varepsilon}}\right)^{2/3} \quad (8)$$

where K_{IC}, r and c respectively denote the fracture toughness of the material, density and dilatational wave speed of the material

Figure 7 shows the above results with the predictions of Equation 6 where Neperian logarithm of the cumulative weight of fragments is plotted against the square root of the fragment size.

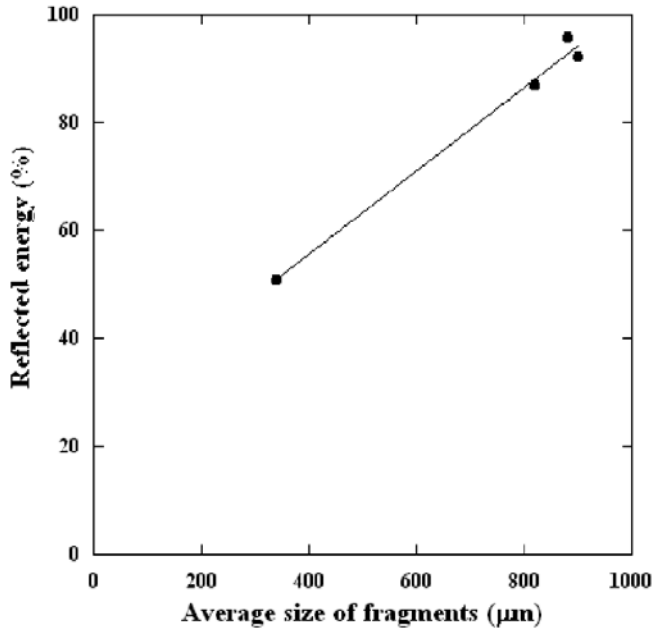

Figure 6. Relationship between SHPB reflected energy and average size of fragments

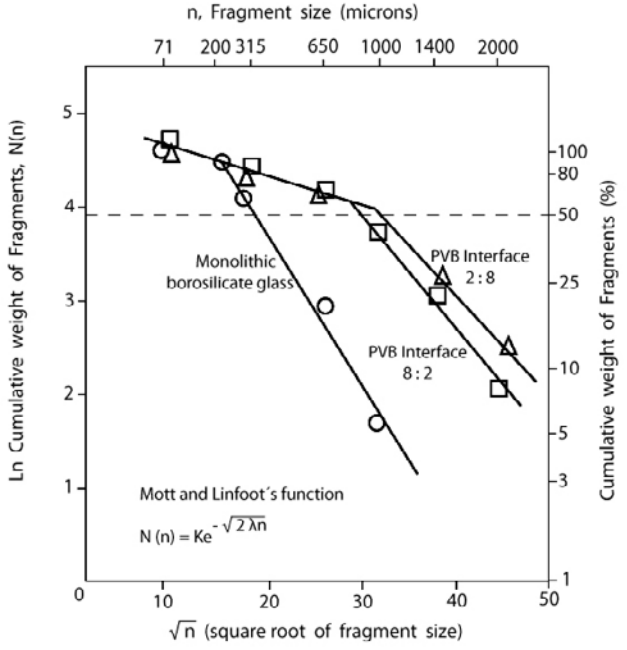

Figure 7. Neperian logarithm of the cumulative weight of fragments against the square root of the fragment size.

As observed the prediction of Mott and Linfoot (eq. 5) provides an adequate fit to the experimental data. Both plots clearly show the laminated samples give rise to higher average fragment sizes than those obtained with monolithic BSG when they are subjected to dynamic fracture using SHPB experiments. Small differences are observed between samples 2:8 and 8:2. According to the predictions of Gray and Kipp given by equation 8, a larger L means a higher dynamic toughness of the laminated samples in relation to monolithic BSG at the same strain rate. The fitting parameter λ from equation 6 can then be associated to the dynamic toughness of the sample.

5. CONCLUSIONS

Several conclusions can be drawn from the dynamic behaviour of the laminate borosilicate glasses studied

1.- The mechanical response under impact loads by means of dynamic compression tests performed in a split Hopkinson pressure bar (SHPB) shows a different behaviour between BSG monoliths and laminates.
2.- The stress-strain curves of the laminates at high strain rates always show a lower strain and a higher yield stress for monolithic BSG.
3.- The borosilicate monolithic reflects much less energy than any of the interlayer laminates; but it absorbs more than any of the others.
4.- The nearer the PVB is to the impact side, the smaller the energy transmitted. Unlike that, the characteristic stress, there are not appreciable differences between the different laminates.
5.- The nearer the PVB is to the impact side, the larger the fragment size and therefore the larger toughness of the laminate
6.- A nearly linear relationship between reflected energy (%) and average fragment size is observed.
7.- The analysis of the SHPB recovered fragments also show that the prediction of the Mott and Linfoot´ statistical function provides an adequate fit to the experimental data. Bimodal distributions were found.

REFERENCES

1. W.A.Gooch. Overview of ceramic armour applications. *Ceramic transactions,Vol 134. 3-21. Ceramic Armour materials by design. Edited by M.McCauley et al. American Ceramic Society,Westerville.Ohio,2001*
2. W.A.Gooch. Overview of the development of ceramic armour technology-Past, present and the future. Presentationat the 30th international conference on advanced ceramics and composites. American Ceramic Society Cocoa Beach, FL,January 22-27,2006
3. M.L.Wilkins R.L.Landingham and C.A.Honodel. Fifth progress report of light armour program. UCRL-50694.Lawrance Radiation Laboratory,1971
4. R.Klement, S. rolc, R. Mikulikova, J. Krestan. Transparent armour materials. J Am Ceram Soc 28, 1091-1095 (2008).
5. E. Straßburger. Ballistic testing of transparent armour ceramics. Journal of the European Ceramic Society 29 (2009) 267–273
6. Sigalas, A. H. Ras,, K. Naidoo** and M.Herrmann . The use of hard and ultrahard ceramics in transportation and security application. *Global Roadmap for Ceramics – ICC2 Proceedings* Verona, June 29-July 4, 161-170, 2008
7. P. J. Patel, G.A. Gilde, P. G. Dehmer and J. W. McCauley Transparent Armor. AMPTIAC. NewsletterVol 4 Num 3.Fall 2000.
8. W.W.Chen, A.M.Rajendran, B.Song and X.Nie. Dynamic fracture of ceramics in armour applications. *J.Am.Ceram.Soc 90, 1005-18 (2007)*
9. D.J.Frew, M.J.Forrester, and W.Chen. Pulse shaping techniques for testing brittle materials with a split Hopkinson pressure bar. *Experimental Mechanics., 42,93-106 (2002)*
10. J.M.Staechler, W.W.Predebon, B.J.Pletka and J.Landford. Testing of high-strength ceramics with the split Hopkinson pressure bar. *J.Am.Ceram.Soc 76, 536-538 (1993).*
11. X. Nie and W.W. Chen. Dynamic failure of borosilicate glass under compressive/shear loading experiments. *J.Am.Ceram.Soc 90, 2556-62 (2007)*
12. T.Jiao,Y.Li,K.T.Ramesh and A.A.Wereszczak. *Int.J.Appl.Ceram.Technol. 1,243-53 (2004)*
13. B.Paliwal,K.T.Ramesh and J.W.McCauley. Direct observation of the dynamic compressive failure of a transparent polycrystalline ceramic (ALON) *J.Am.Ceram.Soc 89, 2128-33, (2007)*
14. P.S. Follansbee.The Hopkinson bar. *Metals handbook, Vol 8, 198-203(1985). Ed. American Society of metals.Ohio*
15. M.A.Martinez, I.S.Chocron, J.Rodriguez, V.Sánchez Gálvez and L.A.Sastre. Confined compression of elactic adhesives at high rates of strain. International Journal of Adhesion and Adhesives 18,375-83 (1998
16. G.Subhash, S.Maiti, P.Geubelle, and D.Ghosh. Recent advances in dynamic indentation fracture, impact damage and fragmentation of ceramics. *J. Am. Ceram. Soc.*, 91, 2777-91 (2008)
17. D.E. Grady and M.E. Kipp. Mechanisms of dynamic fragmentation. Factors governing fragment size. *Mech. Mater.*, 4, 311-20 (1985)
18. D.A.Shockey. Discussion of mechanisms of dynamic fragmentation. Factors governing fragment size. *Mech. Mater.*, 4, 321-24 (1985).
19. A.R. Keller and M. Zhou. Effect of microstructure on dynamic failure resistance of titanium diboride / alumina ceramics. *J. Am. Ceram. Soc.*, 86, 449-57 (2003)
20. C.C. Lienau. Random fracture of a brittle solid. J.Franklin Inst., 221, 485-94 (1936)
21. N.F.Mott and E.H.Linfoot. Ministry of supply, Report AC 3348 (1943)
22. D.E.Grady. Particle size statistics in dynamic fragmentation. J.ApplPhys. 68,6099-105 (1990)
23. D.E Grady and M.E.Kipp. Geometric statistics and dynamic fragmentation. J.Appl.Phys. 58, 1210-22 (1985)

Recibido: 28-9-09
Aceptado: 10-11-09